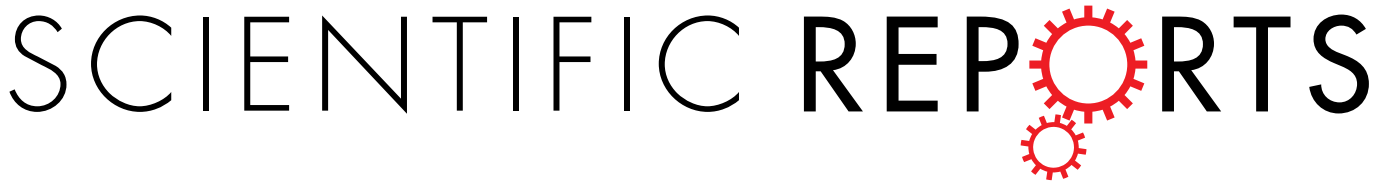

OPEN

Alkanols inhibit voltage-gated K^+ channels via a distinct gating modifying mechanism that prevents gate opening

Received: 24 June 2015
Accepted: 28 October 2015
Published: 30 November 2015

Evelyn Martínez-Morales, Ivan Kopljar†, Dirk J. Snyders & Alain J. Labro

Alkanols are small aliphatic compounds that inhibit voltage-gated K^+ (K_v) channels through a yet unresolved gating mechanism. K_v channels detect changes in the membrane potential with their voltage-sensing domains (VSDs) that reorient and generate a transient gating current. Both 1-Butanol (1-BuOH) and 1-Hexanol (1-HeOH) inhibited the ionic currents of the *Shaker* K_v channel in a concentration dependent manner with an IC_{50} value of approximately 50 mM and 3 mM, respectively. Using the non-conducting *Shaker*-W434F mutant, we found that both alkanols immobilized approximately 10% of the gating charge and accelerated the deactivating gating currents simultaneously with ionic current inhibition. Thus, alkanols prevent the final VSD movement(s) that is associated with channel gate opening. Applying 1-BuOH and 1-HeOH to the *Shaker*-P475A mutant, in which the final gating transition is isolated from earlier VSD movements, strengthened that neither alkanol affected the early VSD movements. Drug competition experiments showed that alkanols do not share the binding site of 4-aminopyridine, a drug that exerts a similar effect at the gating current level. Thus, alkanols inhibit *Shaker*-type K_v channels via a unique gating modifying mechanism that stabilizes the channel in its non-conducting activated state.

Alkanols (or 1-alcohols) are small volatile aliphatic compounds that partition rapidly across the plasma membrane and have the potential to induce anesthesia at high doses[1]. Alkanols have been shown to target both cytoplasmic and plasma membrane proteins[2,3], including voltage-gated K^+ (K_v) channels[4]. K_v channels play an important role in cellular excitability as they constitute the cell's repolarizing power; they shape the action potential duration and help setting the threshold for initiating one.

K_v channels are assembled from four α-subunits, each containing six transmembrane segments (S1–S6) whereby the S5–S6 segments create the K^+ pore[5]. K^+ flow through this pore is controlled by a channel gate that is located in the lower carboxyl-terminal part of S6 ($S6_c$)[6]. Via an electromechanical coupling, composed of the S4–S5 linker and $S6_c$, opening and closure of the channel gate is controlled by the four voltage-sensing domains (VSD) that consist of the S1–S4 segments. Upon changes in the membrane potential, the positively charged residues on the S4 segment (gating charges) move across the plasma membrane generating a transient 'gating current' (I_G)[7,8]. In the generally accepted gating scheme for *Shaker*-type K_v channels, the four VSDs move in a largely independent way from their inward facing rested state to their outward facing activated configuration[9–11]. This transition(s) carries approximately 90% of the total gating charge but does not open the channel gate. Once all four VSDs have reached their activated state, channel gate opening proceeds in a subunit-concerted manner which is accompanied by

Laboratory for Molecular Biophysics, Physiology and Pharmacology, Department of Biomedical Sciences, University of Antwerp, Antwerp, 2610, Belgium. †Present address: Discovery Sciences, Janssen Research and Development, Beerse, 2340, Belgium. Correspondence and requests for materials should be addressed to A.J.L. (email: alain.labro@uantwerpen.be)

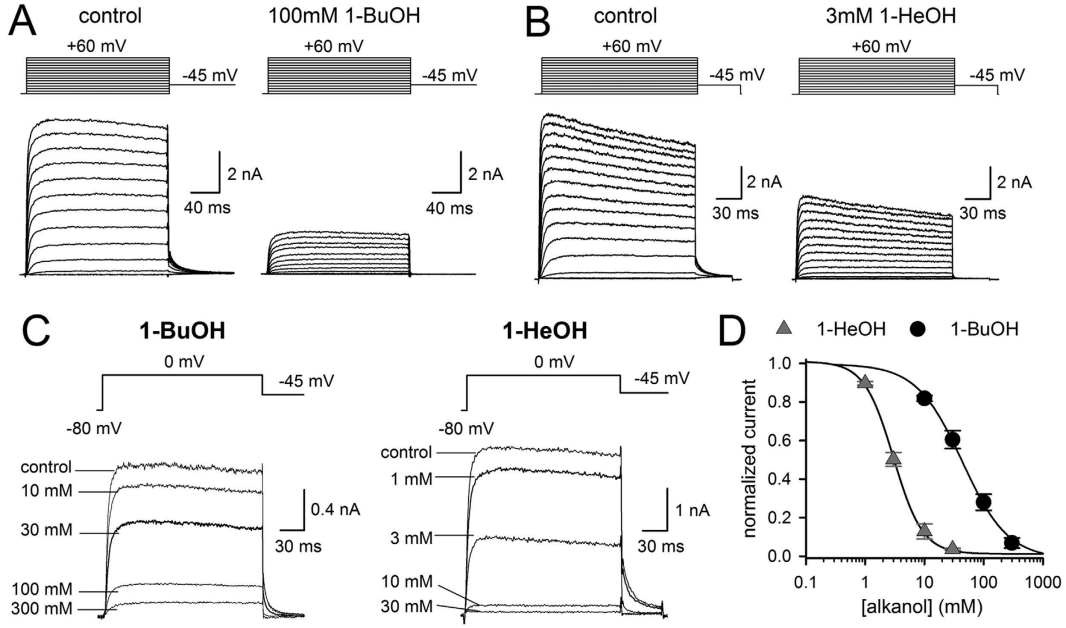

Figure 1. Inhibition of *Shaker*-IR by 1-BuOH and 1-HeOH. (**A**) Representative I_K recordings of *Shaker*-IR in control condition (left) and in presence of 100 mM 1-BuOH (right) elicited by applying depolarization steps from a -80 mV holding potential (pulse protocols are shown on top). (**B**) I_K recordings of *Shaker*-IR obtained in control conditions (left) and in presence of 3 mM 1-HeOH (right). (**C**) Steady-state I_K recordings (elicited with a voltage step from -80 mV to 0 mV) upon wash-in of different concentrations of 1-BuOH (left) and 1-HeOH (right). Establishment of channel inhibition was monitored by repetitive pulsing to 0 mV. (**D**) Concentration-response curves obtained by plotting the normalized steady-state I_K amplitude at 0 mV, determined from I_K recordings as shown in panel C, as a function of 1-BuOH (circles, $n = 5$) or 1-HeOH (triangles, $n = 7$) concentration. Solid lines represent the average fit with a Hill function.

moving the last 10% of the gating charge[12–14]. Furthermore, channel gate opening stabilizes the VSD in its outward facing activated state and is manifested in slower VSD deactivation kinetics[10,15].

Analyzing the sensitivity of different K_v channels to alkanols revealed an inter-species difference wherein the K_v channels from the fruit fly *drosophila melanogaster* displayed a higher affinity than their mammalian orthologs[16,17]. The higher alkanol sensitivity of the *drosophila Shaw*2 channel could be transplanted onto its mammalian K_v3.4 counterpart by exchanging the S4–S5 linker[18]. Site-specific residue substitution studies further supported that the S4–S5 linker forms with possible contribution of $S6_c$ a key determinant in channel inhibition by alkanols[4,19–22]. To elucidate alkanols' mechanism of action, we performed detailed gating current analysis of the *drosophila Shaker* K_v channel and show that 1-Butanol (1-BuOH) and 1-Hexanol (1-HeOH) stabilize the channel in the non-conducting activated state, which results in a 10% reduction in gating charge movement and an accelerated VSD deactivation. Although this behavior was reminiscent to the effect of 4-aminopyridine (4-AP)[14,23], alkanols act via a distinct binding site for preventing the *Shaker* K_v channel of passing the final subunit-concerted transition leading to channel opening.

Results

Concentration-dependent inhibition of Shaker K_v channel by 1-BuOH and 1-HeOH. The *drosophila Shaw2* K_v channel was identified to display the highest sensitivity for alkanols and has therefore been the subject to study the mechanism of their action[4,16,19,21]. The *drosophila Shaker* K_v channel was also inhibited by alkanols but compared to *Shaw2* it displayed a lower sensitivity[17]. Since its cloning, the *Shaker* K_v channel became rapidly the prototypical K_v channel for structure-function studies and most of the current knowledge on the operation of the VSDs, the electromechanical coupling and the channel gate is based on studies in this channel. Thus, despite its lower sensitivity, the available knowledge on the gating mechanism is an advantage of the *Shaker* K_v channel for determining the mechanism of channel inhibition by alkanols.

Alkanols are classified in short chain (up to 5 carbonyls, C1 to C5) or long chain (C6 – C22) 1-alcohols[24]. In this study, 1-BuOH and 1-HeOH were chosen as representative compounds of a short and long chain alkanol. Their effect was tested on both the ionic (I_K) and gating (I_G) currents of the fast (N-type) inactivation removed *Shaker*-IR channel. At the I_K level, *Shaker*-IR was inhibited by both 1-BuOH and 1-HeOH in a concentration-dependent manner (Fig. 1A–C). For 1-BuOH a concentration-response curve was obtained with an IC_{50} value of 51.8 ± 5.9 mM ($n = 5$) and a Hill coefficient of 0.92 ± 0.04 (Fig. 1D).

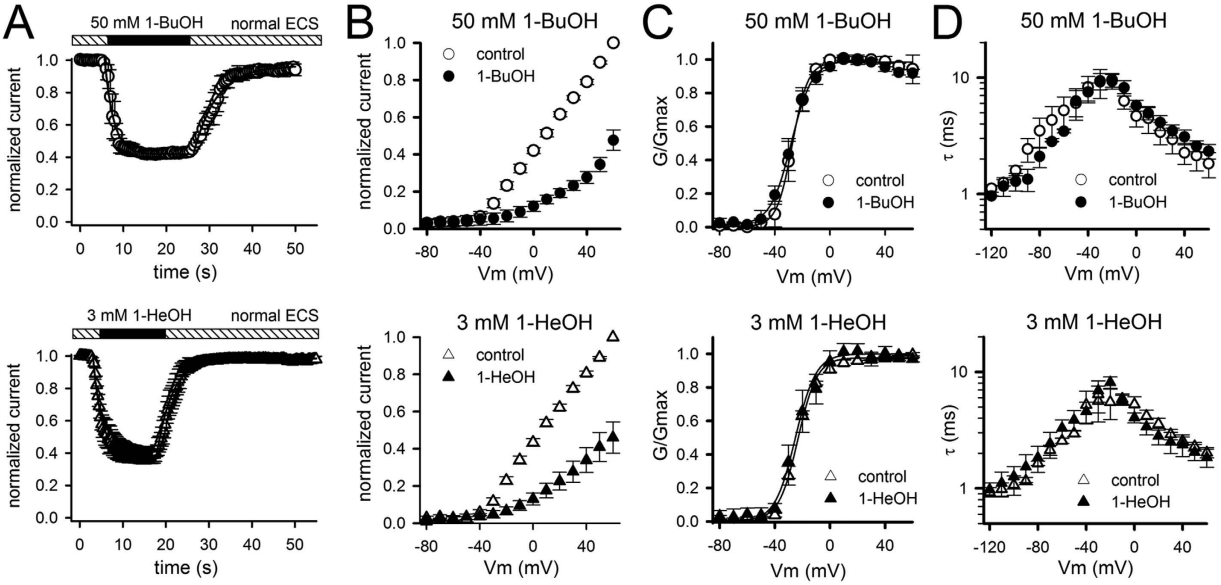

Figure 2. Alkanols inhibited I_K without affecting the kinetics. (**A**) Monitoring the inhibition in I_K during application of 50 mM 1-BuOH (top panel) or 3 mM 1-HeOH (bottom panel) indicated that the I_K inhibition developed rapidly with a time constant of 5.2 ± 1.2 s ($n = 8$) and 3.7 ± 0.7 s ($n = 9$) for 1-BuOH and 1-HeOH respectively. The I_K inhibition was fully reversible upon wash-out of both alkanols and the current recovery was relatively fast yielding time constants of 7.6 ± 2.1 s ($n = 8$) and 4.8 ± 1.7 s ($n = 9$) for 1-BuOH and 1-HeOH respectively. (**B**) Normalized peak current versus voltage relationships, obtained from pulse protocols shown in Fig. 1A, in control conditions (open symbols) and presence of 50 mM 1-BuOH (top panel, $n = 5$) or 3 mM 1-HeOH (bottom panel, $n = 6$). (**C**) Normalized conduction versus voltage GV curves in control conditions (open symbols) and presence of 50 mM 1-BuOH (top panel, $n = 5$) or 3 mM 1-HeOH (bottom panel, $n = 6$). Solid lines represent the average fit with a Boltzmann equation ($V_{1/2}$ and slope factor values are provided in Table 1). (**D**) Time constants of I_K activation (τI_{Kac}) and deactivation (τI_{Kdeac}) in control conditions (open symbols) and in presence of 50 mM 1-BuOH (top panel, $n = 7$) or 3 mM 1-HeOH (bottom panel, $n = 8$).

1-HeOH had a slightly higher affinity and yielded a concentration-response curve with an IC_{50} value of 2.7 ± 0.2 mM ($n = 7$) and a Hill coefficient of 1.13 ± 0.22 (Fig. 1D). Monitoring the development of I_K inhibition and analyzing the remaining steady-state I_K amplitude upon application of 50 mM 1-BuOH or 3 mM 1-HeOH (IC_{50} concentrations) indicated that: (1) the I_K inhibition developed rapidly and was fully reversible upon wash-out of both alkanols, and (2) both alkanols did not induce major alterations in the voltage dependence of channel opening nor the time constants of channel activation (τI_{Kac}) and deactivation (τI_{Kdeac}) (Fig. 2 and Table 1). An apparent channel inactivation behavior or rising phase in the deactivating (I_{Kdeac}) tail current (i.e. a hooked tail), which are typical hallmarks for an open channel blocker, were not observed (Fig. 1A–C). Thus, 1-BuOH and 1-HeOH inhibited the I_K amplitude without affecting the kinetics, and both compounds achieved this through a mechanism most likely different from open channel block, as proposed previously[4].

1-BuOH and 1-HeOH accelerate VSD deactivation and immobilize approximately 10% of the gating charge. The I_K measurements only report on the final opening of the channel gate, which is an end state in the activation pathway from closed to open. From I_G analysis it has been reported that the VSD traverses at least one non-conducting activated state before the channel gate opens. Channel gate opening subsequently slows down VSD deactivation[10,15], which can be visualized by gradually prolonging the duration of the depolarizing pre-pulse (Fig. 3A). Thus, to assess whether 1-BuOH and 1-HeOH affect transitions early in the activation pathway, i.e. before the channel gate opened, we tested the effect of both compounds on the I_G recordings of the non-conducting *Shaker*-IR pore mutant W434F[25]. During wash-in of both 1-BuOH and 1-HeOH we noted a concentration-dependent acceleration of the deactivating (I_{Gdeac}) gating currents (Fig. 3B,C). Plotting the time constant of VSD deactivation (τI_{Gdeac}, obtained by fitting the decaying phase of I_{Gdeac}) as a function of 1-BuOH or 1-HeOH concentration yielded concentration-response curves with IC_{50} values of 67 ± 1 mM ($n = 10$) and 3.0 ± 0.4 mM ($n = 6$), and Hill coefficients of 1.3 ± 0.4 and 1.6 ± 0.3, respectively (Fig. 3D).

To examine whether this acceleration in τI_{Gdeac} was associated with a reduction in gating charge movement, we integrated the activating (I_{Gac}) gating currents (elicited during the depolarizing test pulse)

	GV curve *(voltage dependence of gate opening)*				
Shaker-IR	$V_{1/2}$ (mV)	*k* (mV)			*n*
control conditions	−27.0 ± 1.3	5.6 ± 0.7			11
1-BuOH (50 mM)	−28.5 ± 2.3	5.1 ± 0.7			5
1-HeOH (3 mM)	−25.4 ± 1.2	7.5 ± 0.9			6
Shaker-IR-P475A	$V_{1/2}$ (mV)	*k* (mV)			*n*
control conditions	74 ± 1	12.3 ± 0.7			8
1-BuOH (300 mM)	50 ± 1	6.8 ± 0.7			4
100 mM	62 ± 1	9.6 ± 0.4			8
1-HeOH (30 mM)	49 ± 1	6.6 ± 0.6			5
10 mM	64 ± 1	10.7 ± 0.6			5
	QV curve *(voltage dependence of VSD movement)*				
Shaker-IR-W434F	$V_{1/2}$ (mV)	*k* (mV)			*n*
control conditions	−33.2 ± 5.4	−11.6 ± 2.0			10
1-BuOH (300 mM)	−32.4 ± 3.4	−12.5 ± 1.7			5
1-HeOH (30 mM)	−31.4 ± 0.9	−10.1 ± 0.8			4
	1st comp		***2nd comp***		
Shaker-IR-W434F-P475A	$V_{1/2}$ (mV)	*k* (mV)	$V_{1/2}$ (mV)	*k* (mV)	*n*
control conditions	−33.1 ± 0.8	14.5 ± 0.8	59.6 ± 2.7	10.1 ± 2.4	8
1-BuOH (300 mM)	−39.2 ± 1.4	16.2 ± 1.2	52.2 ± 1.2	9.1 ± 1.1	5
1-HeOH (30 mM)	−35.3 ± 1.5	16.9 ± 1.5	50.2 ± 1.1	3.6 ± 1.4	4

Table 1. Midpoint ($V_{1/2}$) and slope factor (*k*) values of the GV and QV curves of *Shaker*-IR, *Shaker*-IR-P475, and their non-conducting W434F variants.

after reaching steady-state modification of the τI_{Gdeac} kinetics. This analysis indicated that there was an alkanol-dependent reduction in gating charge movement concomitantly with the acceleration in τI_{Gdeac}. The reduction in total gating charge as a function of alkanol concentration yielded for 1-BuOH and 1-HeOH concentration-response curves with IC_{50} values of 88 ± 2 mM ($n = 10$) and 13.8 ± 1.6 mM ($n = 6$), and Hill coefficients of 1.5 ± 0.2 and 1.5 ± 0.2, respectively (Fig. 3E). Based on these concentration-response curves, the maximal reduction in charge movement amounted to approximately 10% and 12% upon application of 300 mM 1-BuOH and 30 mM 1-HeOH, respectively.

To determine the kinetics and voltage dependence of VSD activation, we applied incremental depolarizing voltage steps starting from a constant hyperpolarized initial voltage (activation protocol, Fig. 4A). To characterize VSD deactivation adequately, a deactivation pulse protocol was used (Fig. 4B). Integrating the I_{Gac} recordings, obtained in control conditions and after steady-state 1-BuOH and 1-HeOH modification, yielded charge vs. voltage QV curves (Fig. 4C). Interestingly, the QV curves determined in presence of 1-BuOH or 1-HeOH displayed $V_{1/2}$ and slope factor values similar as in control condition (Table 1). This indicated that neither alkanol affected the voltage dependence of the remaining gating charge movement. As noted during the wash-in protocol (Fig. 3B,C), both alkanols accelerated τI_{Gdeac} without markedly altering the I_{Gac} kinetics (τI_{Gac}, Fig. 4D,E). Thus, both alkanols accelerated τI_{Gdeac} and immobilized approximately 10% of the gating charge movement but did not affect the voltage dependence of the early VSD movements. These observations indicated that in presence of 1-BuOH or 1-HeOH the *Shaker* channel is able to reach the non-conducting activated state but it cannot pass the subunit-cooperative step leading to channel gate opening. Accordingly, the τI_{Gdeac} values in presence of saturating alkanol concentrations should corresponded to τI_{Gdeac} in control conditions when the activating pre-pulse is very short and channels only reach the non-conducting activated state. In control conditions τI_{Gdeac} amounted at −120 mV to 0.32 ± 0.03 ms ($n = 6$) upon a brief 0.5 ms depolarization, determined from pulse protocols shown in Fig. 3A. In presence of 300 mM 1-BuOH or 30 mM 1-HeOH τI_{Gdeac} at −120 mV were 0.48 ± 0.08 ms ($n = 4$) and 0.53 ± 0.10 ms ($n = 4$) respectively (Fig. 4D,E), which are indeed similar to the value in control conditions.

1-alkanols and 4-AP have different binding sites but immobilize the same gating charge component. The impact of 1-BuOH and 1-HeOH on the I_G recordings of the *Shaker*-IR-W434F channel

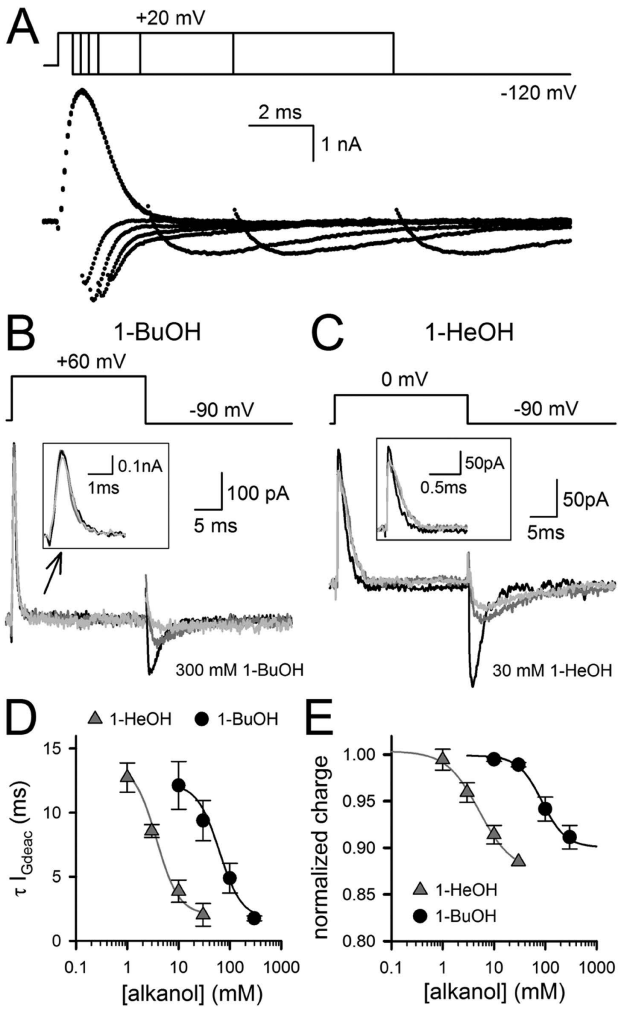

Figure 3. Impact of alkanols on I_G recordings of *Shaker*-IR-W434F. (**A**) Representative I_G recordings of *Shaker*-IR-W434F recorded in control conditions with the pulse protocol shown on top. Note that prolonging the depolarization at +20 mV gradually slowed down I_{Gdeac} upon repolarization to −120 mV. (**B**) Superposition of *Shaker*-IR-W434F steady-state I_G recordings in control condition (gray) and in presence of 100 mM (dark gray) and 300 mM (black) 1-BuOH. Inset shows a scale up view of I_{Gac}. Note the gradual acceleration in I_{Gdeac} upon application of higher concentrations of 1-BuOH. (**C**) Superposition of steady-state I_G recordings in control condition (gray) and in presence of 3 mM (dark gray) and 30 mM (black) 1-HeOH. (**D**) Concentration-response curves obtained by plotting the weighted τI_{Gdeac} at −90 mV (obtained from I_{Gdeac} recordings shown in panel A and B) as a function of 1-BuOH (circles, $n = 10$) or 1-HeOH (triangles, $n = 6$) concentration. (**E**) Concentration-response curves obtained by plotting the normalized charge movement, which was determined by integrating the steady-state I_{Gac} recordings and normalizing the calculated charge to the total charge moved in control condition, as a function of alkanol concentration.

was reminiscent of the effect of 4-AP that prevents the channels from passing the late subunit-cooperative step of channel gate opening, resulting in a similar 10% reduction in gating charge movement[14]. To assess if 4-AP and 1-BuOH immobilized the same gating charge component, we determined the reduction in gating charge movement using a mixture of 1 mM 4-AP and 300 mM 1-BuOH, which for both compounds are saturating concentrations. First, we applied 1 mM 4-AP that resulted in an approximately 10% loss of gating charge movement and an acceleration of τI_{Gdeac}, as has been described before[14,23]. After establishing a steady-state 4-AP effect, we applied 300 mM 1-BuOH in the continued presence of 1 mM 4-AP. The addition of 1-BuOH did not result in an extra reduction of gating charge movement or further acceleration of the I_{Gdeac} kinetics (Fig. 5). This indicated that both compounds affected the same gating charge component and further supported that alkanols stabilize the channel in the non-conducting activated state similar to 4-AP.

Although alkanols and 4-AP exert a similar effect at the gating current level, they may act through different binding sites. Whereas the binding site of 4-AP partially overlaps with that of internal pore

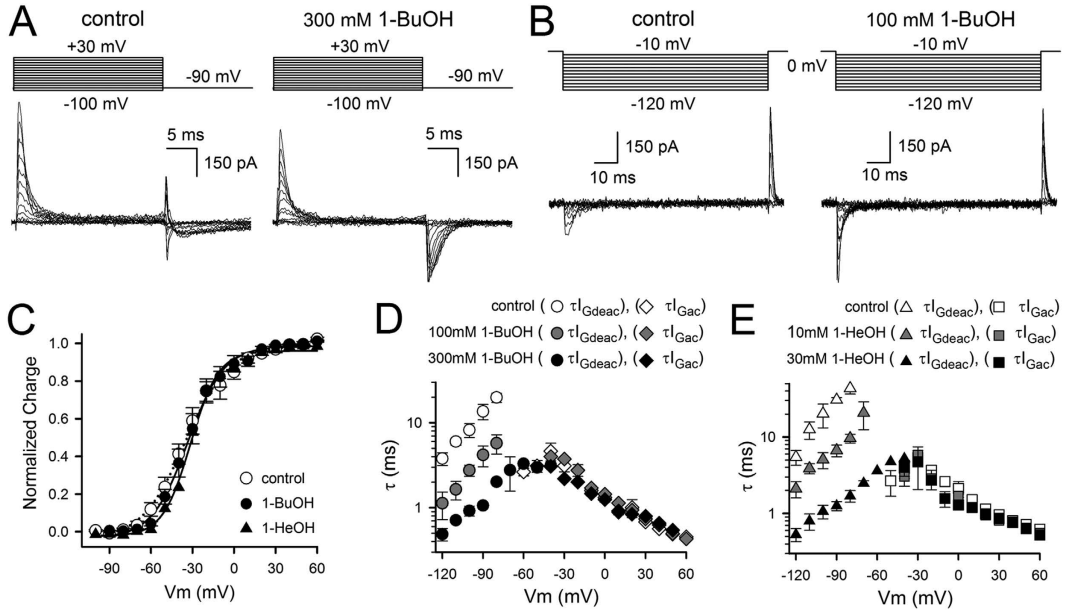

Figure 4. Biophysical properties of *Shaker*-IR-W434F upon alkanol application. (**A**) Representative I_{Gac} recordings of *Shaker*-IR-W434F in control condition (left) and in presence of 300 mM 1-BuOH (right) elicited using the pulse protocols shown on top. (**B**) Representative I_{Gdeac} recordings elicited with the deactivation pulse protocols shown on top; in control conditions (left) and in presence of 100 mM 1-BuOH (right). Inter-sweep holding potential was −90 mV and the depolarizing pre- and post-pulse to 0 mV were 15 ms in duration. (**C**) Charge vs. voltage QV curves in control condition (white circles, $n = 10$) and in presence of 300 mM 1-BuOH (black circles, $n = 5$) or 30 mM 1-HeOH (black triangles, $n = 4$) were created by plotting the normalized charge (obtained from integrating I_{Gac} recordings from pulse protocols shown in panel A) as a function of voltage. Curves shown are the average fit to a Boltzmann equation. (**D**) Time constants of VSD activation (τI_{Gac}) in control condition (white diamonds, $n = 8$) and in presence of 100 mM (gray diamonds, $n = 3$) or 300 mM (black diamonds, $n = 5$) 1-BuOH. For VSD deactivation the weighted τI_{Gdeac} kinetics are shown. Note the gradual acceleration in τI_{Gdeac} between control (white circles), 100 mM 1-BuOH (gray circles) and 300 mM 1-BuOH (black circles). (**E**) Panel shows the voltage-dependent τI_{Gac} kinetics in control condition (white squares, $n = 7$) and in presence of 10 mM (gray squares, $n = 3$) or 30 mM (black squares, $n = 4$) 1-HeOH. Similar to 1-BuOH the τI_{Gdeac} kinetics accelerated in presence of 10 mM (gray triangles, $n = 3$) and 30 mM 1-HeOH (black triangles, $n = 4$), control conditions (white triangles).

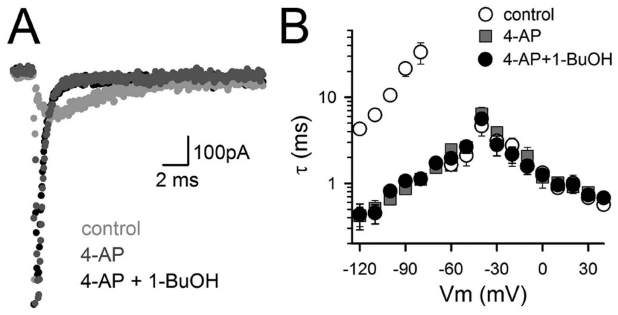

Figure 5. 1-BuOH and 4-AP immobilize the same gating charge component. (**A**) Superposition of steady-state I_{Gdeac} recordings of *Shaker*-IR-W434F, elicited during a repolarizing step to -120 mV upon a 50 ms depolarization at 0 mV, in control condition (light gray), in presence of 1 mM 4-AP (dark gray), and in presence of 1 mM 4-AP plus 300 mM 1-BuOH (black). Note that the mixture of 4-AP plus 1-BuOH did not result in an extra acceleration of I_{Gdeac} decay or an extra reduction in gating charge movement. (**B**) Panel shows τI_{Gac} and τI_{Gdeac} in control condition (white circles, $n = 6$), in presence of 4-AP (dark gray squares, $n = 5$), and 4-AP plus 1-BuOH mixture (black circles, $n = 6$). Both drug conditions resulted in a similar acceleration of τI_{Gdeac} without affecting τI_{Gac} markedly.

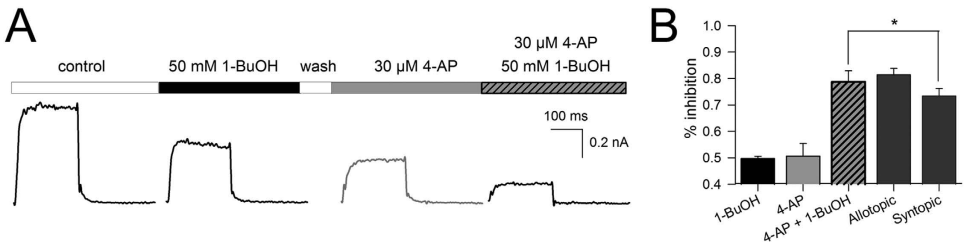

Figure 6. 1-BuOH and 4-AP do not compete for inhibiting *Shaker*-IR. (**A**) Sequentially recorded I_K of *Shaker*-IR in control condition and after steady-state inhibition by 50 mM 1-BuOH and 30 μM 4-AP. Finally, instead of washing the 30 μM 4-AP out, a mixture of 30 μM 4-AP plus 50 mM 1-BuOH was added and the amount of I_K inhibition was determined. (**B**) Bar chart shows the average reduction in $I_K \pm$ S.E.M. ($n = 7$) after applying 50 mM 1-BuOH, 30 μM 4-AP and the mixture of both compounds (30 μM 4-AP plus 50 mM 1-BuOH). The percentage of I_K inhibition was calculated by normalizing the steady-state I_K in presence of drug to the I_K amplitude in control conditions. The expected reduction in I_K for an allotopic and syntopic model was calculated as described in Material and Methods. Note, the experimentally obtained value differed only statistically from the predicted value of a syntopic model (*$p < 0.05$).

blockers[26,27], alkanols have been proposed to target the electromechanical coupling that is located outside the K^+ pore. To test whether 4-AP and 1-BuOH have structurally different binding sites, we performed drug competition experiments using IC_{50} concentrations of 4-AP (30 μM) and 1-BuOH (50 mM). After establishing approximately 50% steady-state I_K inhibition with 4-AP, we applied a mixture of 30 μM 4-AP and 50 mM 1-BuOH. This mixture resulted in $78.7 \pm 4.1\%$ ($n = 7$) inhibition of I_K (Fig. 6), thus yielding an additional inhibition of 29% in I_K amplitude compared to each compound separately.

To evaluate whether 4-AP and 1-BuOH competed, the expected inhibition of the mixture was calculated using a syntopic (both compounds compete) or an allotopic (no competition) model[28]. Using an allotopic model and the experimentally determined inhibition of each compound separately, the predicted inhibition of the mixture was $81.4 \pm 2.4\%$ ($n = 7$). With a syntopic model the predicted inhibition was $73.4 \pm 2.8\%$ ($n = 7$). Because the experimentally determined inhibition (78.7%) differed only statistically ($p < 0.05$) from the predicted value of the syntopic model (Fig. 6), our data matched best an allotopic model indicating that there was no competition between both compounds.

1-BuOH and 1-HeOH activate the Shaker-IR-P475A mutant by accelerating channel opening. A previous study reported that substituting a highly conserved proline residue in the $S6_c$ of the *Shaw2* channel (the second proline of a highly conserved PXP motif within the $S6_c$ of K_v channels) by a neutral amino acid such as alanine inverted the effect of the alkanols[22]. Thus, instead of inhibiting the channel mutant, application of alkanols potentiated the current amplitude. An alanine substitution for the corresponding proline (P475) in *Shaker*-IR shifted the threshold for channel opening towards more depolarized potentials by affecting the late step(s) of channel gate opening while leaving earlier VSD transitions unaffected[29]. Consequently, the *Shaker*-IR-P475A mutant displays slow I_{Kac} kinetics that is only weakly voltage-dependent.

Applying 1-BuOH or 1-HeOH to the *Shaker*-IR-P475A mutant resulted in a concentration-dependent increase in I_K and an acceleration of $\tau\ I_{Kac}$ (Fig. 7A,B), which is in agreement with previous data obtained in the *Shaw2* channel[22]. With higher concentrations of 1-BuOH or 1-HeOH the typical conduction versus voltage GV curves, which were determined from normalizing the deactivation tail current of activation protocols (Fig. 8A), appeared to become steeper and to shift slightly towards more hyperpolarized potentials (Fig. 8B, Table 1). However, concomitantly with the accelerated τI_{Kac} kinetics, also the inactivation process became more pronounced and the peak I_K amplitude started to decrease at higher alkanol concentrations (Fig. 7A,B). Therefore, the small hyperpolarizing shift and steepening of the GV curves could be an apparent effect due to the accelerated channel inactivation. To test this possibility, we determined the normalized conduction G from the peak outward currents using the Goldman-Hodgkin-Katz current equation. The GV curves obtained with this approach, which should be less sensitive to inactivation, were in presence of alkanols similar to those in control conditions (Fig. 8B). Thus, although both compounds resulted in I_K activation, neither 1-BuOH nor 1-HeOH affected the voltage dependence of channel opening substantially. To evaluate if the pronounced channel inactivation behavior reflects in fact open channel block, we examined I_{Kdeac} more closely. In contrast to what is expected with open channel block, the I_{Kdeac} recordings did not cross nor did they display a noticeable hook (Fig. 7A,B). In fact, the τI_{Kdeac} kinetics accelerated markedly which suggested that also the accelerated channel inactivation was due to gating modification. All these effects were fully reversible upon wash-out of both alkanols.

The I_{Kac} of *Shaker*-IR-P475A displayed two components and was best approximated with a double exponential function yielding a fast and a slow τI_{Kac} component[29]. However, the fast component contributed only marginally to the overall I_K amplitude and the weighted τI_{Kac} kinetics approximated the value of the slow component in control condition (Fig. 8C). 1-BuOH or 1-HeOH accelerated channel

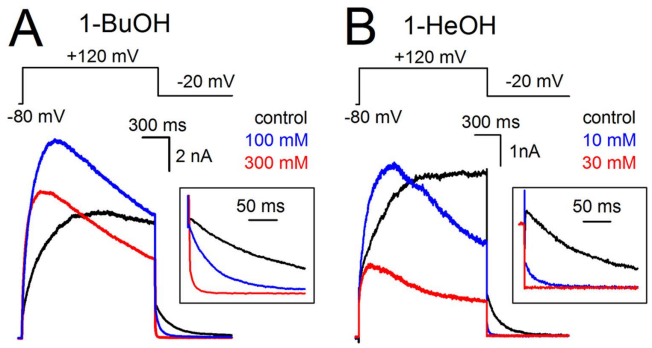

Figure 7. Alkanol-dependent activation of *Shaker*-IR-P475A. (**A**) Steady-state I_K recordings of *Shaker*-IR-P475A in control condition (black), 100 mM (blue), and 300 mM (red) 1-BuOH elicited using the pulse protocol shown on top. (**B**) Steady-state I_K recordings obtained in control condition (black), 10 mM (blue) and 30 mM 1-HeOH (red). In presence of alkanols the currents activated markedly faster and current inactivation was more pronounced. Insets show scale up views of the deactivating (I_{Kdeac}) tail currents.

opening markedly but approximating the I_{Kac} currents with a double exponential function indicated that the time constants of both the fast and slow component were similar to those obtained in control condition. However, the contribution of the fast component in the total current amplitude increased as a function of alkanol concentration (Fig. 8C). Consequently, the weighted τI_{Kac} accelerated with increasing alkanol concentration (Fig. 8D,E). Similar to I_{Kac}, the weighted τI_{Kdeac} kinetics, obtained from fitting I_{Kdeac} with a double exponential function, accelerated in an alkanol concentration-dependent manner (Fig. 8D,E). Plotting the weighted τI_{Kac} as a function of 1-BuOH or 1-HeOH concentration yielded concentration-response curves with IC_{50} values of 58.8 ± 3.0 mM ($n = 5$) and 4.6 ± 0.8 mM ($n = 4$), and Hill coefficients of 1.5 ± 0.4 and 1.3 ± 0.3, respectively (Fig. 8F). This indicated that the alanine substitution for P475 in $S6_c$ did not affect the affinity for alkanols, suggesting that the conformation of the binding site remained intact.

1-BuOH and 1-HeOH did not affect the VSD movements of the P475A mutant. Since the *Shaker*-IR-P475A mutant did not affect the early VSD movements, the QV curve was split and displayed two gating charge components whereby the late one corresponded with the voltage dependence of channel gate opening[29]. Analyzing the gating currents of *Shaker*-IR-W434F-P475A in presence of 300 mM 1-BuOH or 30 mM 1-HeOH indicated that the voltage dependence of neither the early nor the late gating charge component was affected by 1-BuOH or 1-HeOH (Fig. 9 and Table 1). This was in agreement with the absence of an obvious shift in the threshold of channel opening (Fig. 8B). Also the I_{Gac} time constants, which in *Shaker*-IR-W434F-P475A report directly on the kinetics of the early VSD movements[29], were unaffected by 1-BuOH or 1-HeOH. These I_G data confirmed that 1-BuOH and 1-HeOH did not affect the voltage-dependent transitions of the *Shaker*-IR-P475A mutant but facilitated a late largely voltage-independent transition in the activation pathway, a transition that is compromised by the P475A mutation.

Discussion

1-BuOH and 1-HeOH inhibited the *Shaker*–IR channel in a concentration-dependent manner without displaying the classic hallmarks of an open channel blocker. Therefore, alkanols appear to act as gating modifiers that stabilize the channels in a non-conducting state[4]. To elucidate which state is stabilized by alkanols, we determined the impact of 1-BuOH and 1-HeOH on the I_G recordings of *Shaker*-IR-W434F. Both alkanols caused a concentration-dependent reduction in gating charge movement associated with accelerated VSD deactivation (Fig. 3). This data indicated that alkanols interfere with the transition from the non-conducting activated conformation to full channel gate opening, which occurs in a highly subunit-cooperative (concerted) manner. Consequently, the reduction in either I_K or gating charge movement as a function of alkanol concentration yielded concentration-response curves with similar IC_{50} values and Hill coefficients (Figs 1,3). Since alkanols have been proposed to operate via the S4-S5 linker[18], there are 4 potential alkanol binding sites on the channel that appear to operate largely independently (Hill coefficients of approximately 1). As they interfere with a subunit-cooperative transition, binding of a single alkanol molecule (occupying only one out of four binding sites) can be sufficient to prevent channel gate opening and losing about 10% of the gating charge movement. Accordingly, a previous study, which used concatemeric constructs, showed that channels with less than four high affinity binding sites (e.g. only 2) were still inhibited by alkanols[4]. Thus, we propose that alkanols inhibit *Shaker*-IR currents by preventing the channels of passing the final concerted step in the activation sequence that opens the channel gate. Therefore, the ionic current data analysis represented in figure 2 reports on the channels

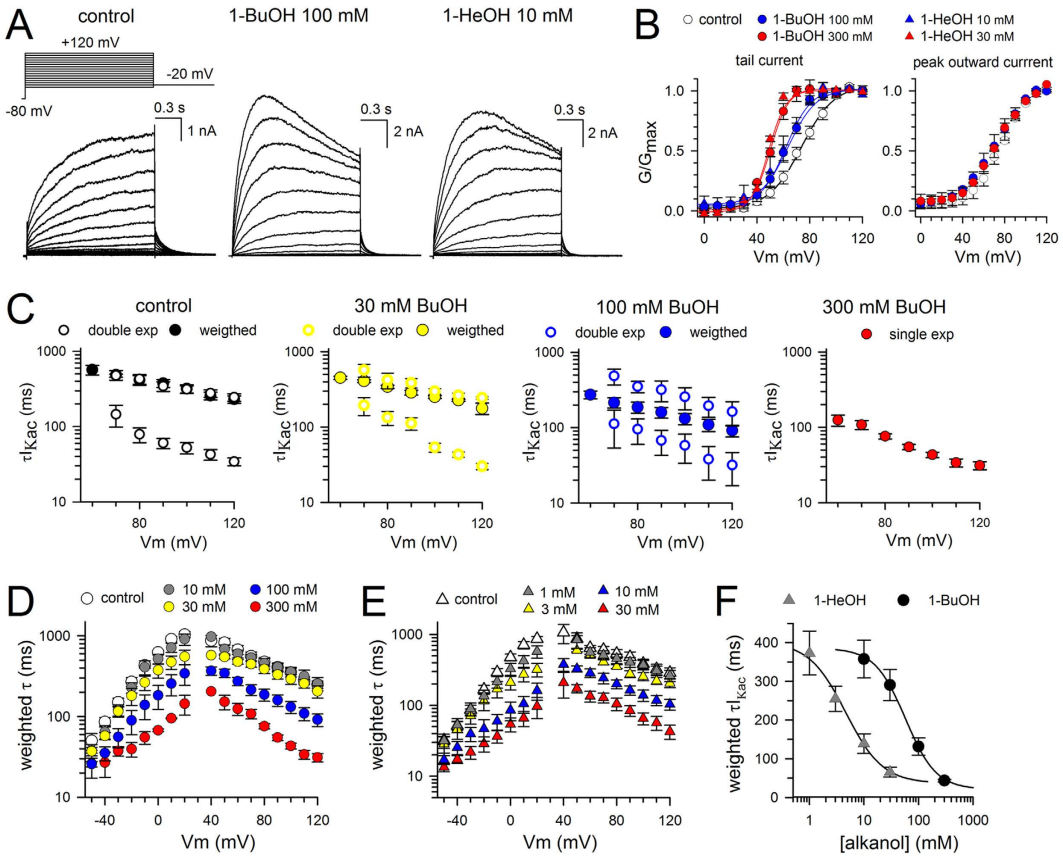

Figure 8. Biophysical properties of *Shaker*-IR-P475A upon alkanol application. (**A**) Representative I_{Kac} recordings of *Shaker*-IR-P475A in control conditions, 100 mM 1-BuOH and 10 mM 1-HeOH, elicited using the pulse protocol shown on top. (**B**) Conduction vs. voltage GV curves of *Shaker*-IR-P475A in control conditions (white circles), 100 mM 1-BuOH (blue circles), 300 mM 1-BuOH (red cricles), 10 mM 1-HeOH (blue triangles), and 30 mM 1-HeOH (red triangles). GV curves displayed in the left panel were obtained by normalizing tail current amplitudes. Solid lines represent the average fit with a Boltzmann equation ($V_{1/2}$ and slope factor values are provided in Table 1). Right panel displays the GV curves determined from analyzing the peak outward currents. (**C**) Panels from left to right show the τI_{Kac} values of *Shaker*-IR-P475A upon increasing 1-BuOH concentrations with the left most panel showing the values in control conditions. The fast and slow τI_{Kac} components are represented with open symbols and the weighted τI_{Kac} with filled symbols. Note that the contribution of the fast τI_{Kac} component increased upon higher 1-BuOH concentrations; compare weighted τI_{Kac} values in 30 mM (yellow symbols) and 100 mM (blue symbols). In presence of 300 mM 1-BuOH (red symbols) only the fast component could be resolved and I_{Kac} was approximated with a single exponential function. (**D**) Plot shows the weighted τI_{Kac} and τI_{Kdeac} values in control conditions (white) and in presence of 10 mM (gray, $n = 4$), 30 mM (yellow, $n = 5$), 100 mM (blue, $n = 8$), and 300 mM (red, $n = 4$) 1-BuOH. (**E**) Plot shows the effect of 1 mM (gray, $n = 7$), 3 mM (yellow, $n = 9$), 10 mM (blue, $n = 5$), and 30 mM (red, $n = 5$) 1-HeOH on the weighted τI_{Kac} and τI_{Kdeac} kinetics. (**F**) Concentration-response curves obtained by plotting the weighted τI_{Kac} at +100 mV as a function of 1-BuOH (black circles, $n = 10$) and 1-HeOH (gray triangles, $n = 6$) concentration. Solid lines represent the fit with a Hill equation.

that were free of alkanols which explains why both the normalized GV curves (Fig. 2C) and the kinetics (Fig. 2D) in presence of alkanols were similar to control conditions.

The impact of 1-BuOH and 1-HeOH on *Shaker*'s gating charge movement was reminiscent to that of the well-characterized drug 4-AP[14], and both compounds stabilize the *Shaker* K_v channel in the non-conducting activated state. However, both compounds achieve this by acting via distinct binding sites (Fig. 6). Whereas the binding determinants for 4-AP, including those for guanidine compounds that possibly work in a similar manner[30], reside within $S6_c$[31,32], alkanols are suggested to distort the coupling between the S4-S5 linker and $S6_c$[33]. The observation that alkanols rescued partly the kinetics of the *Shaker*-IR-P475A mutant, favors the idea that alkanols alter the conformation of the S4–S5 linker and/or $S6_c$ without disrupting their communication completely. By altering the conformation of the

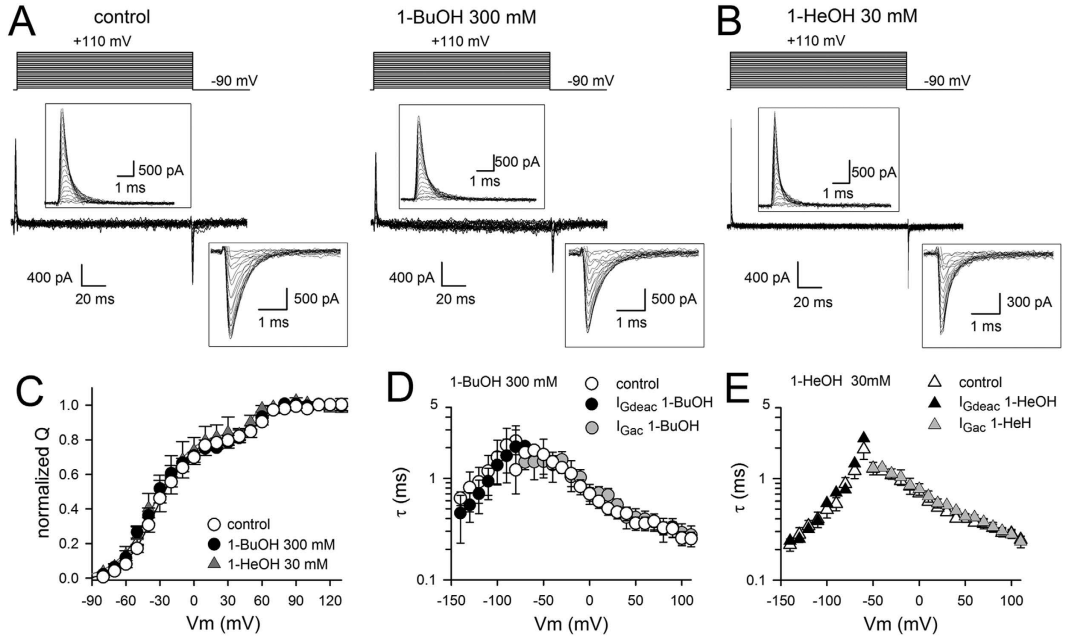

Figure 9. Alkanols did not affect the I_G behavior of *Shaker*-IR-W434F-P475A. (**A**) Representative I_G recordings of *Shaker*-IR-W434F-P475A recorded in control condition (left recordings) and after approximately 10 minutes wash-in of 300 mM 1-BuOH (right recordings), elicited with the pulse protocols shown on top. Insets show scale up views of I_{Gac} and I_{Gdeac} respectively. (**B**) Representative I_G recordings of *Shaker*-IR-W434F-P475A in presence of 30 mM 1-HeOH. (**C**) QV curves of *Shaker*-IR-W434F-P475A in control conditions (white circles) and presence of 300 mM 1-BuOH (black circles, $n = 5$) or 30 mM 1-HeOH (gray triangles, $n = 4$). (**D**) τI_{Gac} (gray circles) and τI_{Gdeac} (black circles) kinetics of *Shaker*-IR-W434F-P475A in presence of 300 mM 1-BuOH, which were similar to the kinetics in control condition (white circles). (**E**) Similar to 1-BuOH, 30 mM 1-HeOH did not affect the τI_{Gac} (gray triangles) or the τI_{Gdeac} (black triangles) kinetics compared to control condition (white triangles).

S4-S5 linker and/or $S6_c$, the electromechanical coupling is compromised as its operation relies on a correct positioning of both segments with respect to each other[34].

Mutations that affect the communication between the VSD and the channel gate might therefore alter the alkanol effect, as is the case in *Shaker*-IR-P475A. Apparently, 1-BuOH and 1-HeOH did not shift the voltage dependence of the late gating charge component in *Shaker*-IR-P475A (Fig. 9), which is expected if the mutation was only to affect the equilibrium constant of the transition from the non-conducting activated to the open state. Therefore, the structural consequences of the P475A mutation should be more severe and the *Shaker*-IR-P475A mutant displayed, accordingly, a biphasic current activation that in absence of alkanols is dominated by the slow component. We propose that alkanol binding to the *Shaker*-IR-P475A channel alters the conformation of the S4-S5 linker and/or its communication with $S6_c$ (as it does in WT *Shaker*-IR), and in doing so it coincidentally restores the conformation of the $S6_c$ channel gate that is compromised by the mutation. Alkanols then act as activators of the *Shaker*-IR-P475A mutant by yielding I_K current activation that is dominated by the fast component (Fig. 8C–E), thus accelerating a late largely voltage-independent transition of channel gate opening. Notably, the effect of both 1-BuOH and 1-HeOH on the *Shaker*-IR-P475A mutant was comparable to the behavior of poly-unsaturated-fatty acids (PUFAs): accelerating channel opening followed by more pronounced channel inactivation at higher concentrations (Fig. 7A,B). PUFAs have been shown to alter the kinetics of K_v channels leading to current activation or current inhibition, in part by accelerating the inactivation process[35]. At low concentrations several PUFAs act as channel activators but at higher concentrations they result in channel inhibition[36–38]. Whereas their activating property is ascribed to their ability to shift the voltage dependence of channel opening towards more hyperpolarized potentials and to facilitate the late subunit-concerted transition of channel opening[39,40], their molecular mechanism to induce channel inhibition is still debated[41]. Whereas alkanols most likely target the S4-S5 linker of K_v channels[33], PUFAs supposedly exert their effect through the VSD[39,40], although a role for the S4-S5 linker has been suggested[42].

Alkanols and 4-AP immobilize the same VSD movement(s) in the *Shaker*-IR channel (Fig. 5), but both compounds achieve this via distinct drug binding sites (Fig. 6) and a different mechanism of action. This conclusion is further supported by the observation that the mutant *Shaker*-IR-P475A is activated by alkanols (Figs 7,8) but is insensitive to 4-AP[29]. The presence of other (possibly overlapping) intracellular or lipid-accessible binding sites for gating modifying compounds is supported by: (1) the finding that the

gating modifier toxin gambierol occupies a lipid exposed S5-S6 crevice outside the K^+ pore[43], a binding site which is most likely shared by psora compounds[44] and (2) the observation that ruthenium complexes uncouple VSD movement from channel gate opening but in contrast to alkanols they immobilize about 50% of the gating charge[45]. Furthermore, the binding site for the volatile anesthetic halothane has been shown to overlap with that of alkanols[21], and both isoflurane and servoflurane, which belong to the same class of halogenated general anesthetics, potentiate K_v channels instead of inhibiting them[46–48].

The intoxicating and sedating effects of exposure to high alkanol concentrations are well described and ion channels (including K_v channels) do most likely form one of their molecular targets. We provide a mechanistic basis for understanding their effect on K_v channels and show that 1-BuOH and 1-HeOH interfere directly with the gating apparatus of the *Shaker*–IR K_v channel. They inhibit *Shaker*-IR by stabilizing the non-conducting activated state preventing the channels from passing the final subunit-concerted transition leading to channel gate opening. They achieve this through a unique gating modifying mechanism different from that of 4-AP. Our findings strengthen the idea that there exist different intracellular drug binding sites that via distinct mechanisms of action exert a similar gating modifying effect; this opens new possibilities for designing modulators of K_v channels.

Methods

Molecular Biology. The N-terminal deletion Δ6–46 *Shaker* clone (*Shaker*-IR), which removes fast inactivation[49], was used in this study. The W434F mutation, which yields a non-conducting *Shaker*-IR-W434F channel[25], and the P475A mutation were introduced as described previously[29]. All channel constructs were expressed using a pGW1 expression vector. The plasmid that codes for the green fluorescent protein, used to identify transfected cells, was purchased from Clontech (Palo Alto, CA, USA). Plasmid DNA for mammalian expression was obtained by amplification in XL2 Bluescript cells (Stratagene), and afterwards isolated using the endotoxin-free Maxiprep kit (Macherey-Nagel, Düren, Germany). The cDNA concentration was determined by UV absorption.

Cell culture. HEK293 cells were cultured in Modified Eagle's Medium (MEM) supplemented with 10% fetal bovine serum, 1% penicillin/streptomycin and 1% non-essential amino acids (Invitrogen, Carlsbad, CA, USA). Cells were transiently transfected with the appropriate channel DNA plasmids using polyethyleneimine that was purchased from Sigma-Aldrich (St Louis, MO, USA), details of procedure was described previously[29].

Electrophysiology. Whole-cell ionic I_K or gating I_G current measurements were done at room temperature (20 to 23 °C) using an Axopatch-200B amplifier and the recordings were digitized with a Digidata-1200 A acquisition system (Molecular Devices, Sunnyvale, CA, USA). Both I_K and I_G recordings were digitized at 10 kHz sampling rate after passing a 5 KHz Bessel low-pass filter. Command voltages and data storage were controlled with pClamp10 software. Patch pipettes were pulled from 1.2 mm quick-fill borosilicate glass capillaries (World Precision Instruments, Sarasota, FL, USA) with a P-2000 puller (Sutter Instrument Co., Novato, CA, USA) and afterwards heat-polished, to have patch pipettes with a resistance of approximately 1.5 MOhm determined with the filled pipette in the bath solution.

For I_K measurements the cells were constantly superfused with external bath solution that contained (in mM) NaCl 130, KCl 4, $CaCl_2$ 1.8, $MgCl_2$ 1, HEPES 10, Glucose 10, adjusted to pH 7.35 with NaOH. The patch pipettes were filled with internal solution containing (in mM) KCl 110, K_4BAPTA 5, K_2ATP 5, $MgCl_2$ 1, HEPES 10, adjusted to pH 7.2 with KOH. For I_G measurements the monovalent cations were replaced with N-methyl-D-glucamine (NMG^+). The bath solution contained (in mM) NMG^+ 140, HEPES 10, Glucose 10, $MgCl_2$ 1, $CaCl_2$ 1.8, titrated to pH 7.35 with HCl. The pipette solution contained (in mM) NMG^+ 140, HEPES 10, EGTA 10, $MgCl_2$ 1, titrated to pH 7.2 with HCl. Junction potentials were zeroed with the filled pipette in the bath solution and experiments were excluded from analysis if the voltage error estimate exceeded 5 mV after series resistance compensation. For I_G measurements, leak currents and remaining capacitive currents were subtracted online using a −P/6 protocol (using a holding potential of −95 mV). I_K recordings were not leak corrected.

Drug solutions. 1-BuOH and 1-HeOH (Sigma-Aldrich, St. Louis, MO, US) were directly dissolved in the external recording solution for either I_K or I_G measurements. The different test concentrations were daily made as both compounds are volatile lowering the effective concentration upon storage. For the highest concentration of 1-BuOH tested (300 mM), the osmolarity of the extracellular solution for I_K or I_G recordings increased by approximately 300 mOsm resulting in a total osmolarity of ~640 mOsm. Because of the rapid partitioning of alkanols across the plasma membrane, we expected a minor impact of this increase in osmolarity. Indeed, the cells tolerated remarkably well the perfusion of the 300 mM 1-BuOH solution. This was not the case when the cells were perfused with a 600 mOsm extracellular solution that contained glucose, which does not easily partition across the plasma membrane, to increase osmolarity (data not shown). 4-AP was purchased from Sigma-Aldrich and after dissolving it in the external recording solutions the pH was adjusted to 7.35 using HCl. All compounds were applied to the cells using a pressurized fast perfusion system equipped with a quartz micromanifold (ALA scientific, Farmingdale, NY, USA), allowing rapid exchange of the external solutions.

Data analysis. Details of pulse protocols used to elicit I_K or I_G recordings were adjusted to determine the biophysical properties of each construct adequately and are shown in the figures or described in legends. All the graphs were built using SigmaPlot 11.0 (Systat Software Inc., San Jose, CA, USA). If not mentioned otherwise, the conductance vs. voltage (GV) curves were determined from analyzing normalized tail current amplitudes and the charge vs. voltage (QV) curves by integrating the activating I_G currents. The QV and GV curves of *Shaker*-IR were fitted with a Boltzmann equation: $y = 1/\{1 + \exp[-(V - V_{1/2})/k]\}$, where V represents the applied voltage, $V_{1/2}$ the midpoint potential at which 50% of the total charge has moved or half of the channels have opened, and k the slope factor. For the P475A mutant the GV curve was also approximated with a single Boltzmann equation whereas its QV curve was approximated with the sum of two Boltzmann distributions. Activation I_K kinetics (τI_{Kac}) were determined by approximating the rise in I_{Kac} with a single or double exponential function. Deactivation I_K kinetics (τI_{Kdeac}) were obtained from single or double exponential fits to the I_{Kdeac} decay elicited at various repolarizing potentials following a 25 ms depolarizing pre-pulse to + 20 mV that activated the channels. When a double exponential function was used to determine the fast (τ_{fast}) and slow (τ_{slow}) component of the τI_{Kac} and τI_{Kdeac} kinetics, the weighted time constants (τ_W) were calculated based on the amplitude of each component: $\tau_W = (A_{fast}/(A_{fast} + A_{slow}))$ x $\tau_{fast} + (A_{slow}/(A_{fast} + A_{slow}))$ x τ_{slow}, with A_{fast} and A_{slow} the amplitude of the fast and slow component respectively. The I_G activation and deactivation kinetics (τI_{Gac} and τI_{Gdeac}) were determined by fitting the decaying part of I_{Gac} and I_{Gdeac} with a single exponential function. All results are expressed as mean ± S.E.M. with n the number of cells analyzed.

Concentration–response curves (both from I_K and I_G analysis) were fitted in the program OriginPro 8 (OriginLab Corp., Northampton, MA, USA) with a Hill equation: $I_{effect} = I_{min} + (\{I_{max} - I_{min}\}/\{1 + ([alkanol]/IC_{50})^{Hill\ coefficient}\})$, where [alkanol] is the concentration of 1-BuOH or 1-HeOH and IC_{50} the concentration that induces 50% effect. To test whether 1-BuOH shares a similar and/or overlapping binding site with 4-AP, we performed competition experiments based on a previously described approach[28]. The method is based on comparing the experimental determined inhibition to the expected level of channel inhibition using an allotopic (non-competing) or a syntopic model (competing). Formulas used for calculating the expected inhibition in presence of both compounds ($I_{NX,Y}$) according to the allotopic and syntopic model were $I_{NX,Y} = (I_{NX} + I_{NY} - I_{NX}I_{NY})$ and $I_{NX,Y} = ((I_{NX} + I_{NY} - 2I_{NX}I_{NY})/(1 - I_{NX}I_{NY}))$, respectively. I_{NX} and I_{NY} were the experimentally determined level of channel inhibition induced by each compound independently. I.e. I_{NX} was the inhibition induced by 1-BuOH and I_{NY} the level of inhibition induced by 4-AP. A two way analysis of variance (ANOVA) was used to determine the differences of a dual inhibition. A *post hoc* Dunnett's was used to compare both models.

References

1. Fang, Z. *et al.* Anesthetic potencies of n-alkanols: results of additivity and solubility studies suggest a mechanism of action similar to that for conventional inhaled anesthetics. *Anesth Analg* **84,** 1042–1048 (1997).
2. Franks, N. P. Molecular targets underlying general anaesthesia. *Br J Pharmacol* **147** Suppl 1, S72–S81 (2006).
3. Franks, N. P. & Lieb, W. R. What is the molecular nature of general anaesthetic target sites? *Trends Pharmacol Sci* **8,** 169–174 (1987).
4. Covarrubias, M., Vyas, T. B., Escobar, L. & Wei, A. Alcohols inhibit a cloned potassium channel at a discrete saturable site. Insights into the molecular basis of general anesthesia. *J Biol Chem* **270,** 19408–19416 (1995).
5. Long, S. B., Tao, X., Campbell, E. B. & MacKinnon, R. Atomic structure of a voltage-dependent K^+ channel in a lipid membrane-like environment. *Nature* **450,** 376–382 (2007).
6. Labro, A. J. & Snyders, D. J. Being flexible: the voltage-controllable activation gate of Kv channels. *Front Pharmacol* **3,** 168 (2012).
7. Seoh, S. A., Sigg, D., Papazian, D. M. & Bezanilla, F. Voltage-sensing residues in the S2 and S4 segments of the *Shaker* K^+ channel. *Neuron* **16,** 1159–1167 (1996).
8. Aggarwal, S. K. & MacKinnon, R. Contribution of the S4 segment to gating charge in the *Shaker* K^+ channel. *Neuron* **16,** 1169–1177 (1996).
9. Zagotta, W. N., Hoshi, T., Dittman, J. & Aldrich, R. W. *Shaker* potassium channel gating II: Transitions in the activation pathway. *J Gen Physiol* **103,** 279–319 (1994).
10. Bezanilla, F., Perozo, E. & Stefani, E. Gating of *Shaker* K^+ channels: II. The components of gating currents and a model of channel activation. *Biophys J* **66,** 1011–1021 (1994).
11. Schoppa, N. E. & Sigworth, F. J. Activation of Shaker potassium channels. III. An activation gating model for wild-type and V2 mutant channels. *J Gen Physiol* **111,** 313–342 (1998).
12. Smith-Maxwell, C. J., Ledwell, J. L. & Aldrich, R. W. Role of the S4 in cooperativity of voltage-dependent potassium channel activation. *J Gen Physiol* **111,** 399–420 (1998).
13. Gagnon, D. G. & Bezanilla, F. A single charged voltage sensor is capable of gating the Shaker K^+ channel. *J Gen Physiol* **133,** 467–483 (2009).
14. Loboda, A. & Armstrong, C. M. Resolving the gating charge movement associated with late transitions in K channel activation. *Biophys J* **81,** 905–916 (2001).
15. Batulan, Z., Haddad, G. A. & Blunck, R. An intersubunit interaction between S4-S5 linker and S6 is responsible for the slow off-gating component in Shaker K^+ channels. *J Biol Chem* **285,** 14005–14019 (2010).
16. Covarrubias, M. & Rubin, E. Ethanol selectively blocks a noninactivating K^+ current expressed in Xenopus oocytes. *Proc Natl Acad Sci USA* **90,** 6957–6960 (1993).
17. Anantharam, V., Bayley, H., Wilson, A. & Treistman, S. N. Differential effects of ethanol on electrical properties of various potassium channels expressed in oocytes. *Mol Pharmacol* **42,** 499–505 (1992).
18. Harris, T., Shahidullah, M., Ellingson, J. S. & Covarrubias, M. General anesthetic action at an internal protein site involving the S4-S5 cytoplasmic loop of a neuronal K(+) channel. *J Biol Chem* **275,** 4928–4936 (2000).
19. Barber, A. F., Liang, Q., Amaral, C., Treptow, W. & Covarrubias, M. Molecular mapping of general anesthetic sites in a voltage-gated ion channel. *Biophys J* **101,** 1613–1622 (2011).
20. Bhattacharji, A. *et al.* The concerted contribution of the S4-S5 linker and the S6 segment to the modulation of a Kv channel by 1-alkanols. *Mol Pharmacol* **70,** 1542–1554 (2006).

21. Bhattacharji, A., Klett, N., Go, R. C. & Covarrubias, M. Inhalational anaesthetics and n-alcohols share a site of action in the neuronal Shaw2 Kv channel. *Br J Pharmacol* **159,** 1475–1485 (2010).
22. Harris, T., Graber, A. R. & Covarrubias, M. Allosteric modulation of a neuronal K^+ channel by 1-alkanols is linked to a key residue in the activation gate. *Am J Physiol-Cell Ph* **285,** C788–C796 (2003).
23. McCormack, K., Joiner, W. J. & Heinemann, S. H. A characterization of the activating structural rearrangements in voltage-dependent Shaker K+ channels. *Neuron* **12,** 301–315 (1994).
24. Carignan, D., Desy, O., Ghani, K., Caruso, M. & de Campos-Lima, P. O. The size of the unbranched aliphatic chain determines the immunomodulatory potency of short and long chain n-alkanols. *J Biol Chem* **288,** 24948–24955 (2013).
25. Perozo, E., MacKinnon, R., Bezanilla, F. & Stefani, E. Gating currents from a nonconducting mutant reveal open-closed conformations in *Shaker* K^+ channels. *Neuron* **11,** 353–358 (1993).
26. Chen, F. P. & Fedida, D. On the mechanism by which 4-Aminopyridine occludes quinidine block of the cardiac K^+ channel, hKv1.5. *J Gen Physiol* **111,** 539–554 (1998).
27. Zhang, H., Zhu, B., Yao, J. A. & Tseng, G. N. Differential effects of S6 mutations on binding of quinidine and 4-aminopyridine to rat isoform of Kv1.4: common site but different factors in determining blockers' binding affinity. *J Pharmacol Exp Ther* **287,** 332–343 (1998).
28. Jarvis, G. E. & Thompson, A. J. A golden approach to ion channel inhibition. *Trends Pharmacol Sci* **34,** 481–488 (2013).
29. Martinez-Morales, E., Snyders, D. J. & Labro, A. J. Mutations in the S6 Gate Isolate a Late Step in the Activation Pathway and Reduce 4-AP Sensitivity in Shaker Kv Channel. *Biophys J* **106,** 134–144 (2014).
30. Kalia, J. & Swartz, K. J. Elucidating the molecular basis of action of a classic drug: guanidine compounds as inhibitors of voltage-gated potassium channels. *Mol Pharmacol* **80,** 1085–1095 (2011).
31. Caballero, N. A., Melendez, F. J., Nino, A. & Munoz-Caro, C. Molecular docking study of the binding of aminopyridines within the K^+ channel. *J Mol Model* **13,** 579–586 (2007).
32. Shieh, C. C. & Kirsch, G. E. Mutational analysis of ion conduction and drug binding sites in the inner mouth of voltage-gated K^+ channels. *Biophys J* **67,** 2316–2325 (1994).
33. Zhang, J., Qu, X., Covarrubias, M. & Germann, M. W. Insight into the modulation of Shaw2 Kv channels by general anesthetics: structural and functional studies of S4-S5 linker and S6 C-terminal peptides in micelles by NMR. *Biochim Biophys Acta* **1828**, 595–601 (2013.).
34. Labro, A. J. *et al.* Kv channel gating requires a compatible S4-S5 linker and bottom part of S6, constrained by non-interacting residues. *J Gen Physiol* **132,** 667–680 (2008).
35. Oliver, D. *et al.* Functional conversion between A-type and delayed rectifier K^+ channels by membrane lipids. *Science* **304,** 265–270 (2004).
36. Honore, E., Barhanin, J., Attali, B., Lesage, F. & Lazdunski, M. External blockade of the major cardiac delayed-rectifier K^+ channel (Kv1.5) by polyunsaturated fatty acids. *Proc Natl Acad Sci USA* **91,** 1937–1941 (1994).
37. McKay, M. C. & Worley, J. F. III Linoleic acid both enhances activation and blocks Kv1.5 and Kv2.1 channels by two separate mechanisms. *Am J Physiol-Cell Ph* **281,** C1277–C1284 (2001).
38. Gubitosi-Klug, R. A. & Gross, R. W. Fatty acid ethyl esters, nonoxidative metabolites of ethanol, accelerate the kinetics of activation of the human brain delayed rectifier K^+ channel, Kv1.1. *J Biol Chem* **271,** 32519–32522 (1996).
39. Borjesson, S. I. & Elinder, F. An electrostatic potassium channel opener targeting the final voltage sensor transition. *J Gen Physiol* **137,** 563–577 (2011).
40. Ottosson, N. E., Liin, S. I. & Elinder, F. Drug-induced ion channel opening tuned by the voltage sensor charge profile. *J Gen Physiol* **143,** 173–182 (2014).
41. Moreno, C., Macias, A., Prieto, A., De La Cruz, A. & Valenzuela, C. Polyunsaturated Fatty acids modify the gating of kv channels. *Front Pharmacol* **3,** 163 (2012).
42. Heler, R., Bell, J. K. & Boland, L. M. Homology model and targeted mutagenesis identify critical residues for arachidonic acid inhibition of Kv4 channels. *Channels* **7,** 74–84 (2013).
43. Kopljar, I. *et al.* A polyether biotoxin binding site on the lipid-exposed face of the pore domain of Kv channels revealed by the marine toxin gambierol. *Proc Natl Acad Sci USA* **106,** 9896–9901 (2009).
44. Marzian, S. *et al.* Side pockets provide the basis for a new mechanism of Kv channel-specific inhibition. *Nat Chem Biol* **9,** 507–513 (2013).
45. Jara-Oseguera, A. *et al.* Uncoupling Charge Movement from Channel Opening in Voltage-gated Potassium Channels by Ruthenium Complexes. *J Biol Chem* **286,** 16414–16425 (2011).
46. Li, J. & Correa, A. M. Single-channel basis for conductance increase induced by isoflurane in Shaker H4 IR K(+) channels. *Am J Physiol-Cell Ph* **280,** C1130–C1139 (2001).
47. Barber, A. F., Liang, Q. & Covarrubias, M. Novel activation of voltage-gated K(+) channels by sevoflurane. *J Biol Chem* **287,** 40425–40432 (2012).
48. Correa, A. M. Gating kinetics of Shaker K+ channels are differentially modified by general anesthetics. *Am J Physiol-Cell Ph* **275,** C1009–C1021 (1998).
49. Hoshi, T., Zagotta, W. N. & Aldrich, R. W. Biophysical and molecular mechanisms of Shaker potassium channel inactivation. *Science* **250,** 533–538 (1990).

Acknowledgements

This work was supported by the Mexican National Council for Science and Technology CONACyT (grant 203936 to E.M-M.); and the Belgian Research Fund Flanders (FWO grant G0433.12N to D.J.S.)

Author Contributions

E.M.-M. conducted the experiments; E.M.-M. and A.J.L. performed data analysis; E.M.-M., I.K., D.J.S. and A.J.L. participated in research design; E.M.-M., I.K., D.J.S. and A.J.L. wrote or contributed to the writing of the manuscript.

Additional Information

Competing financial interests: The authors declare no competing financial interests.

How to cite this article: Martínez-Morales, E. *et al.* Alkanols inhibit voltage-gated K^+ channels via a distinct gating modifying mechanism that prevents gate opening. *Sci. Rep.* **5**, 17402; doi: 10.1038/srep17402 (2015).